



Published in final edited form as:

J Biomol NMR. 2018 April ; 70(4): 205–209. doi:10.1007/s10858-018-0181-6.

TROSY Pulse Sequence for Simultaneous Measurement of the ^{15}N R_1 and $\{^1\text{H}\}$ - ^{15}N NOE in Deuterated Proteins

Paul A. O'Brien and Arthur G. Palmer III

Department of Biochemistry and Molecular Biophysics, Columbia University, 630 West 168th Street, New York, NY 10032

Abstract

A TROSY-based NMR experiment is described for simultaneous measurement of the ^{15}N longitudinal relaxation rate constant R_1 and the $\{^1\text{H}\}$ - ^{15}N nuclear Overhauser enhancement. The experiment is based on the observation that the TROSY mixing pulse sequence element symmetrically exchanges ^1H and ^{15}N magnetizations. The accuracy of the proposed technique is validated by comparison to independent measurements of both relaxation parameters for the protein ubiquitin. The simultaneous experiment is approximately 20-33% shorter than conventional sequential measurements.

Keywords

Dynamics; Longitudinal relaxation; Nuclear Overhauser enhancement; Protein; Spin-lattice relaxation; TROSY

The ^{15}N R_1 and R_2 relaxation rate constants and the steady-state $\{^1\text{H}\}$ - ^{15}N nuclear Overhauser enhancement (NOE) provide vital probes of the picosecond-nanosecond dynamics of backbone amide moieties in proteins ¹. Measurement of these three parameters allows characterization of the spectral density function $\mathcal{J}(\omega)$ at the frequencies 0, ω_N , ω_N , and $\omega_H \pm \omega_N$ (the ^1H single quantum and ^{15}N single quantum frequencies frequently are approximated by a single effective frequency through reduced spectral density mapping) ². Experimental protocols and approaches for data interpretation are well-established ¹; however, particularly as measurements at multiple static magnetic fields become more commonplace ³⁻⁵, maximizing the efficiency of experimental methods remains essential.

Measurement of the steady-state $\{^1\text{H}\}$ - ^{15}N NOE requires two experiments: one in which the ^{15}N steady-state magnetization is measured after irradiation of the ^1H spins (saturated), and a second in which the Boltzmann equilibrium ^{15}N magnetization is measured in the absence of ^1H irradiation (unsaturated or control) ⁶. The ratio of the saturated to the unsaturated intensity is the steady-state $\{^1\text{H}\}$ - ^{15}N NOE. Although simple in the abstract, the steady-state $\{^1\text{H}\}$ - ^{15}N NOE experiment suffers from several factors complicating implementation. Chief among these is the inherent lower experimental sensitivity because starting magnetization originates on the low gyromagnetic ^{15}N nucleus, rather than ^1H as in the R_1 and R_2 experiments. In addition, the recycle delays must be set long enough ($> 7-8/R_1$) to ensure complete recovery of equilibrium magnetization in the unsaturated control experiment. Finally, avoidance of saturation transfer through chemical exchange of labile protons

requires careful manipulations of the water magnetization. Addressing these concerns to ensure accurate steady-state $\{^1\text{H}\}$ - ^{15}N NOE values results in long experimental times.

The TROSY-based NOE pulse sequence ⁷, performed without ^1H irradiation, shows a unique feature: following the t_1 period, a reverse-INEPT block transfers transverse ^{15}N magnetization to ^1H for subsequent detection, and simultaneously transfers longitudinal ^1H magnetization to longitudinal ^{15}N magnetization ⁸. In principle, this polarization-enhanced ^{15}N magnetization could serve as the starting point for another relaxation experiment. In the present work, a second pulse sequence block utilizes this magnetization to measure the ^{15}N R_1 relaxation rate constant. Separate storage of decay curves originating with positive or negative values of the initial longitudinal ^{15}N magnetization also allows the steady-state ^{15}N intensity to be obtained by extrapolation during data analysis, and hence calculation of the $\{^1\text{H}\}$ - ^{15}N NOE. Thus, an independent measurement of the saturated spectrum is not necessary.

The pulse sequence for the proposed experiment is shown in Figure 1 and is based on the TROSY pulse sequences of Bax and coworkers ⁹. The first part of the experiment is the control measurement of equilibrium ^{15}N magnetization. In addition, this sequence transfers longitudinal ^1H magnetization to longitudinal ^{15}N magnetization at the start of the first t_2 acquisition period. Following the t_2 period, two orthogonal ^1H 90° hard pulses are used to purge remaining ^1H magnetization and a composite 0° or 180° ^{15}N pulse is used to generate positive or negative ^{15}N longitudinal magnetization. The inversion-recovery relaxation period consists of repeated [$-180^\circ(^1\text{H})-$] blocks with $\tau = 11$ ms ¹⁰. The ^1H 180° pulses are cosine-modulated I-BURP2 pulses to maintain water magnetization on the +z-axis ¹¹. These ^1H 180° pulses serve two purposes: (i) to remove cross-correlated relaxation effects and (ii) to obtain ^{15}N steady-state magnetization by amide proton saturation. The partially relaxed ^{15}N magnetization is frequency labeled and transferred to ^1H for detection during the second t_2 period. The experiment is performed twice for each R_1 relaxation delay: the control equilibrium ^{15}N free induction decays (FID) are co-added while the R_1 FIDs with positive initial ^{15}N longitudinal magnetization ($I_+(t)$), or negative initial ^{15}N longitudinal magnetization ($I_-(t)$) are stored separately. If the inversion-recovery experiment is performed with N relaxation time points and M scans per complex point in t_1 for each relaxation time point then the final data control unsaturated measurement consists of $2MN$ co-added FIDs per complex point in t_1 . The inversion-recovery curves are fit simultaneously to the equations:

$$\begin{aligned} I_+(T) &= I_{ss} + (I_+(0) - I_{ss})e^{-R_1 T} \\ I_-(T) &= I_{ss} + (-I_-(0) - I_{ss})e^{-R_1 T} \end{aligned} \quad (1)$$

in which I_{ss} and R_1 correspond to the steady-state ^{15}N magnetization intensity, and the longitudinal relaxation rate constant, respectively. The initial magnetizations are treated as local variables, while I_{ss} and R_1 are treated as global parameters. The NOE is calculated as the ratio of I_{ss} and the average intensity of the control experiment, I_0 .

The proposed pulse sequence was used to measure ^{15}N R_1 and steady-state ^{15}N - $\{^1\text{H}\}$ NOE for a 1.0 mM sample of [$\text{U-}^2\text{H}, ^{15}\text{N}$] ubiquitin. Sample temperature was calibrated to 298 K using 98% $^2\text{H}_4$ -methanol¹². Relaxation data were collected at 14.1 T on a Bruker DRX600 console equipped with a triple-resonance z-axis gradient cryogenic probe. Spectra were recorded using 4 scans per complex t_1 point, and $t_2 \times t_1$ of 512×128 complex points. The spectral width was set to $9.3 \text{ kHz} \times 2.4 \text{ kHz}$. Relaxation delays were set to $T = n \times 22 \text{ ms}$, where $n = \{2, 4, 10, 18, 44, 88, 240, 464\}$, giving $T = \{0.044, 0.220, 0.396, 0.968, 1.936, 5.280, 10.208\} \text{ s}$. Spectra were processed using NMRPipe¹³, and in-house Python scripts were used to fit relaxation curves for calculation of R_1 and I_{ss} values. The proposed pulse sequence was validated by comparison with results from independent conventional measurements of ^{15}N R_1 and steady-state ^{15}N - $\{^1\text{H}\}$ NOE using TROSY-based pulse sequences⁹. The conventional NOE experiment used 16 scans per complex t_1 point for the control and the saturated spectra; hard 180° ^1H pulses were used to saturate ^1H magnetization. The conventional R_1 experiment used a recycle delay of 3.5 s, 8 scans per complex t_1 point, and 8 relaxation delays spaced between 0 and 1.6 s. Total acquisition times were 32, 13, and 20 hours for the proposed experiment, conventional NOE experiment, and conventional R_1 experiment, respectively. Experimental uncertainties in relaxation parameters are the standard error in the mean of three replicates.

Figure 2 shows representative R_1 relaxation decay curves for Val 5, Thr 9, Ile 30, and Gly 75, which are located in β -sheet, turn, α -helix, and C-terminal regions of ubiquitin, respectively. The absolute value of the initial magnetization for each set of the R_1 curves differed by approximately 2% intensity, with the $I_+(T)$ curve yielding the larger intensity values. As shown in Figure 3, the R_1 and NOE values from the combined experiment are in excellent agreement with reference TROSY-detected experiments for ubiquitin. Comparison of ^{15}N R_1 values between the two experiments gives a correlation coefficient of 0.974 and an RMSD of 0.032. The mean square errors in the measured R_1 values are 0.012 and 0.010 for the conventional and combined experiments. Comparison of steady-state ^{15}N - $\{^1\text{H}\}$ NOE values gives a correlation coefficient of 0.998 and an RMSD of 0.016. The mean square errors in the measured NOE values are 0.014 and 0.010 for the conventional and combined experiments. Corrected for differences in acquisition times, the NOE values for the conventional and combined experiments have very similar root-mean-square uncertainties of 0.00925 and 0.0102, respectively.

The proposed combined experiment differs from separately acquired NOE and R_1 datasets in three ways. (i) The resonance intensities for the “saturated” spectrum, needed to calculate the NOE, are not directly measured, but are extrapolated during the fitting of the positive and negative R_1 relaxation curves; (ii) longitudinal ^1H magnetization is inverted for a period $\tau + t_1$ prior to the TROSY transfer period; and (iii) non-equilibrium longitudinal ^{15}N magnetization relaxes during the first acquisition t_2 period prior to the start of the R_1 relaxation delay. Monte Carlo simulations of these effects were simulated for a protein with tumbling time 5 ns and 15 ns, using a 600 MHz spectrometer (full protonation was assumed for simplicity, which should give an upper bound on sensitivity differences). Simulations assumed that the conventional NOE experiments were recorded with 32 scans per FID for each of the control and saturated spectra. The combined experiment used 64 scans to measure the control spectrum and simultaneously used $N = 8$ time points to measure R_1 ,

with 4 scans for positive initial ^{15}N magnetization and 4 scans for negative initial magnetization. The simulations indicate that the two different NOE measurements have virtually identical sensitivity per unit time for either the 5 ns and 15 ns rotational diffusion correlation times. The R_1 measurement has a lower precision by 15% and ~10% compared with a conventional experiment measured with the same number of scans and time points, for 5 ns and 15 ns tumbling times, respectively. This difference arises from the small relaxation losses noted above. The precision of the R_1 experiment is ~1%, so these small differences are not a major effect on subsequent data analysis. Notably the simulations show that the values of the NOE and R_1 for the combined experiment are uncorrelated, with $R^2 < 0.01$. The theoretical calculations are in approximate agreement with the experimental results reported for ubiquitin. The combined experiment yields both the NOE and R_1 ; thus, R_1 is obtained essentially for free. The time savings afforded by the combined experiment depends on the relative lengths of the conventional NOE and R_1 experiments. For example, savings in experimental time would be 20 or 33% if the conventional R_1 experiment were to be recorded in 1/4 or 1/2 of the experimental time for the conventional NOE measurement.

We have described a TROSY pulse sequence for simultaneous measurement of the intensity of the Boltzmann equilibrium ^{15}N magnetization and the ^{15}N longitudinal relaxation rate constant R_1 in a single experiment. Long-time plateau values from fitting of the R_1 data serve as proxies for the usual saturated $\{^1\text{H}\}$ - ^{15}N intensity to allow calculation of the steady-state $\{^1\text{H}\}$ - ^{15}N NOE . Measurements of ^{15}N R_1 and steady-state ^{15}N - $\{^1\text{H}\}$ NOE on a ubiquitin sample using both the combined experiment and conventional independent experiments are in very good agreement. The greater efficiency of the proposed pulse sequence should become even more useful for larger bio-molecular systems, for which maximizing sensitivity per unit time is critical.

Supplementary Material

Refer to Web version on PubMed Central for supplementary material.

Acknowledgments

Support from National Institutes of Health grants R01 GM050291 (A.G.P.) and T32 GM008281 (P.A.O.) is acknowledged gratefully. We thank Mark Rance (University of Cincinnati) for helpful discussions. Some of the work presented here was conducted at the Center on Macromolecular Dynamics by NMR Spectroscopy located at the New York Structural Biology Center, supported by a grant from the NIH National Institute of General Medical Sciences (P41 GM118302). A.G.P. is a member of the New York Structural Biology Center.

References

1. Palmer AG NMR characterization of the dynamics of biomacromolecules. *Chem Rev* 104, 3623–40 (2004). [PubMed: 15303831]
2. Peng JW & Wagner G Frequency spectrum of NH bonds in eglin c from spectral density mapping at multiple fields. *Biochemistry* 34, 16733–52 (1995). [PubMed: 8527448]
3. Abyzov A et al. Identification of dynamic modes in an intrinsically disordered protein Using temperature-dependent NMR relaxation. *J Am Chem Soc* 138, 6240–51 (2016). [PubMed: 27112095]
4. Gill ML, Byrd RA & Palmer AG Dynamics of GCN4 facilitate DNA interaction: a model-free analysis of an intrinsically disordered region. *Phys Chem Chem Phys* 18, 5839–49 (2016). [PubMed: 26661739]

5. Hsu A, O'Brien PA, Bhattacharya S, Rance M & Palmer AG Enhanced spectral density mapping through combined multiple-field deuterium $^{13}\text{CH}_2\text{D}$ methyl spin relaxation NMR spectroscopy. *Methods* (2017).
6. Cavanagh J, Fairbrother WJ, Palmer III AG, Rance M & Skelton NJ *Protein NMR Spectroscopy* (Second Edition) 679–724 (Academic Press, Burlington, 2007).
7. Zhu G, Xia Y, Nicholson LK & Sze KH Protein dynamics measurements by TROSY-based NMR experiments. *J Magn Reson* 143, 423–6 (2000). [PubMed: 10729271]
8. Favier A & Brutscher B Recovering lost magnetization: polarization enhancement in biomolecular NMR. *J Biomol NMR* 49, 9–15 (2011). [PubMed: 21190063]
9. Lakomek NA, Ying J & Bax A Measurement of ^{15}N relaxation rates in perdeuterated proteins by TROSY-based methods. *J Biomol NMR* 53, 209–21 (2012). [PubMed: 22689066]
10. Ferrage F, Cowburn D & Ghose R Accurate sampling of high-frequency motions in proteins by steady-state $^{15}\text{N}\{-^1\text{H}\}$ nuclear Overhauser effect measurements in the presence of cross-correlated relaxation. *J Am Chem Soc* 131, 6048–9 (2009). [PubMed: 19358609]
11. Gairi M et al. An optimized method for ^{15}N R_1 relaxation rate measurements in non-deuterated proteins. *J Biomol NMR* 62, 209–20 (2015). [PubMed: 25947359]
12. Findeisen M, Brand T & Berger SA ^1H -NMR thermometer suitable for cryoprobes. *Magn Reson Chem* 45, 175–8 (2007). [PubMed: 17154329]
13. Delaglio F et al. NMRPipe: a multidimensional spectral processing system based on UNIX pipes. *J Biomol NMR* 6, 277–93 (1995). [PubMed: 8520220]

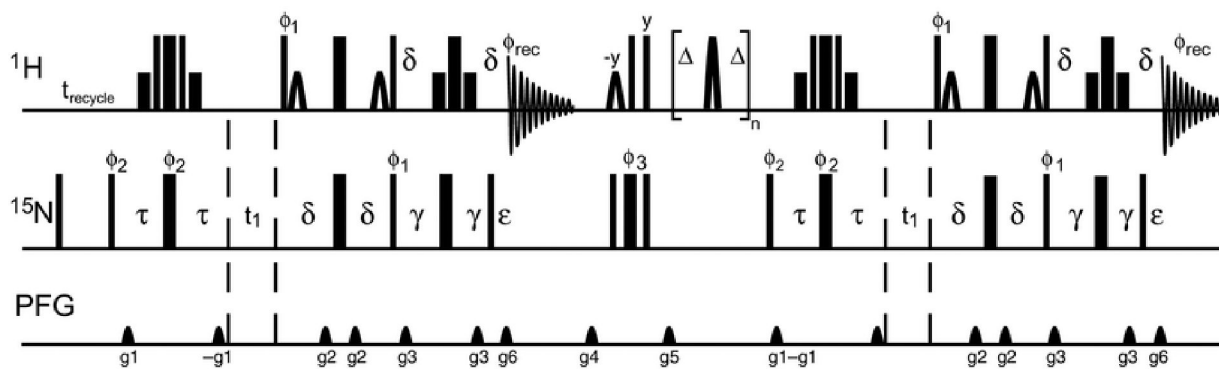


Figure 1.

Pulse sequence for simultaneous measurement of the steady state $\{^1\text{H}\}$ - ^{15}N NOE and the ^{15}N R_1 relaxation rate constant. Thin and thick solid bars represent high-power 90° and 180° pulses, respectively; short open shapes represent water-selective 90° sinc pulses; short thin solid bars represent rectangular water-selective 90° pulses; thick solid bars flanked by two thin bars indicate a 90_x - 210_y - 90_x composite pulse; and the open shaped pulses during the $T = n(2\tau - \tau_{180})$ relaxation period are cosine-modulated I-BURP2 180° pulses of length τ_{180} crafted to leave the water magnetization unperturbed while maximizing inversion of amide protons. Delays: $t_{\text{recycle}} = 11$ s, $\tau = 11$ ms, $\delta = \tau = 2.65$ ms, $\gamma = \delta - \epsilon/2$, and $\epsilon > g_6$. Gradients were applied as square pulses. Gradients g_1 and g_6 were used for coherence selection and other gradients are used for artifact suppression. Gradients: g_1 ($600 \mu\text{s}$, 21.7 G/cm), g_2 ($300 \mu\text{s}$, 6.8 G/cm), g_3 ($1000 \mu\text{s}$, 32.9 G/cm), g_4 ($500 \mu\text{s}$, 6.8 G/cm), g_5 ($1000 \mu\text{s}$, 13.2 G/cm), g_6 ($121.60 \mu\text{s}$, 21.7 G/cm). All pulses are x -phase unless indicated. Phase cycling: $\phi_1 = y$; $\phi_2 = y, -y$, and $\phi_{\text{rec}} = y, -y$. The phase $\phi_3 = y$ for $L(0)$ and $-x$ for $I_+(0)$ in the R_1 experiment. Echo-antiecho selection is obtained by inverting g_1 and ϕ_1 . Pulse sequence and acquisition parameter files are provided as Online Resource 1 and 2, respectively

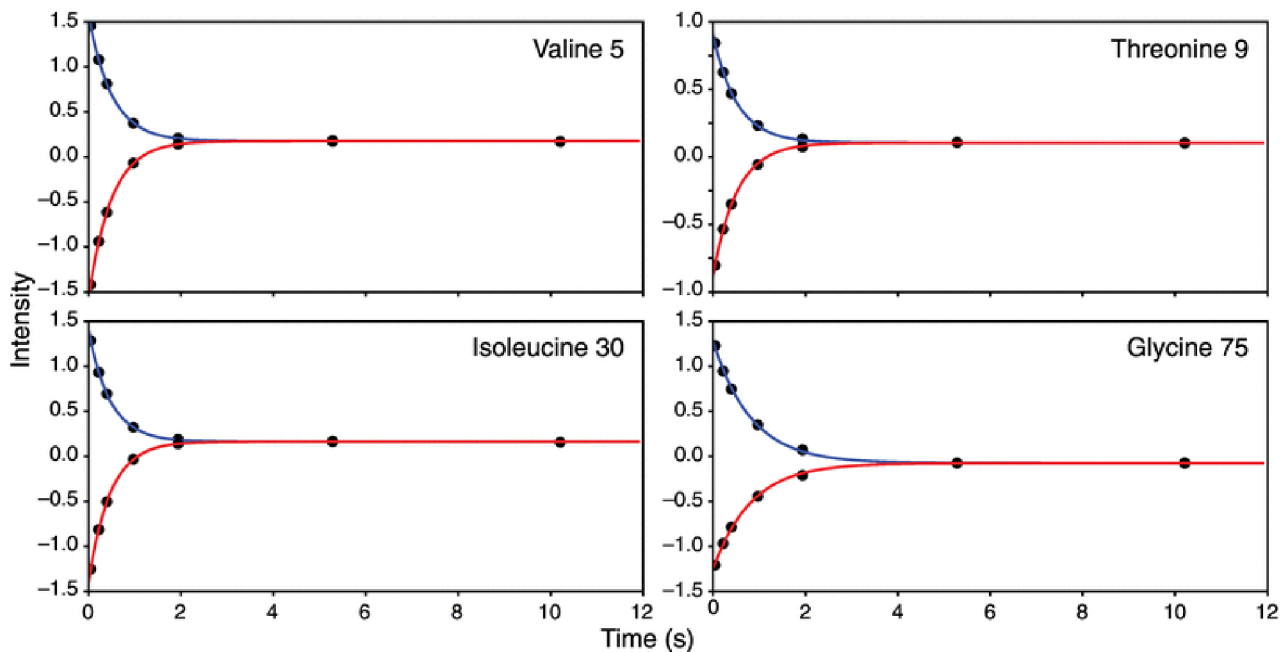


Figure 2.

^{15}N R_1 decay curves for Val 5, Thr 9, Ile 30, and Gly 75 in ubiquitin. Data points and fitted decay curves are shown for (blue) positive ($L_+(T)$) and (red) negative ($L_-(T)$) initial ^{15}N magnetization. Data were fit using Eq. 1 using a Levenberg-Marquardt algorithm. Fitted values for R_1 are (Val 5) 2.001 ± 0.001 , (Thr 9) 1.927 ± 0.016 , (Ile 30) 2.1484 ± 0.016 , and (Gly 75) 797 ± 0.009 (uncertainties are standard error in the mean of three replicates)

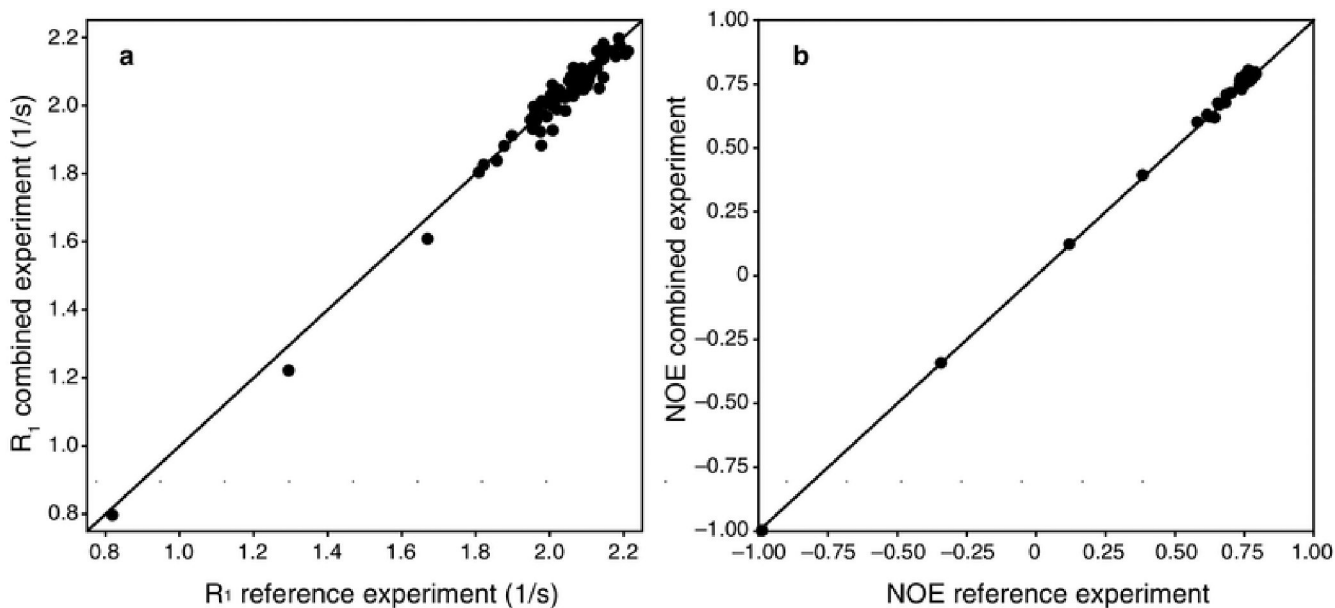


Figure 3.

Comparison of simultaneous and conventional measurements of (a) ^{15}N R_1 relaxation rate constant ($R^2 = 0.974$, RMSD = 0.032) and (b) steady-state $\{^1\text{H}\}$ - ^{15}N NOE ($R^2 = 0.998$, RMSD = 0.016). Uncertainties in measured values are not shown. The mean square errors in the measured R_1 values are 0.012 and 0.010 for the conventional and combined experiments. The mean square errors in the measured NOE values are 0.014 and 0.010 for the conventional and combined experiments. Data values are provided as Online Resource 3